

Stable and metastable freezing of classical correlations in qutrits

C. E. López¹ and F. Lastra²

¹*Departamento de Física, Universidad de Santiago de Chile, USACH, Casilla 307, Correo 2, Santiago, Chile*

²*Departamento de Física, Facultad de Ciencias Básicas, Universidad de Antofagasta, Casilla 170, Antofagasta, Chile*

(Received 8 May 2017; published 11 December 2017)

We study the dynamics of quantum and classical correlations in a two-qutrit system coupled to independent reservoirs. In particular, we address the differences in the dynamics of Markovian and non-Markovian regimes and show that for specific initial states, classical correlations exhibit abrupt changes along the dynamics. A particular sudden change occurs when the classical correlations freeze to a certain value at a given time, revealing the apparition of a pointer-state basis. After this given time, the decoherence only affects quantum correlations. Here we identify two regimes in the decoherence dynamics: a mixed regime when both classical and quantum correlations decay and a quantum regime when only quantum correlations decay. We show that the freezing of classical correlations can be stable or metastable depending on the system-reservoir parameters. In the long-time limit, we find analytical expressions for the pointer-state basis the system settles in and consequently for classical and quantum correlations.

DOI: [10.1103/PhysRevA.96.062112](https://doi.org/10.1103/PhysRevA.96.062112)

I. INTRODUCTION

Quantum to classical transition has been an interesting subject since the beginning of quantum theory [1]. This transition can be described as a flow of correlations from the quantum system to its surroundings [2–4]. Because of that, all correlations that can be shared by two parts cannot be preserved and begin to be lost as time goes by. Recently, characterization of when a quantum system has begun to lose its quantum component has regained the attention of researchers [5–9]. On the other hand, the complexity in the maximization procedure to obtain any correlation shared by the subsystems is well known when the dimension of the Hilbert space is increased more than 2 in each of them. This is a hard task. Indeed, there exist a few cases where analytical expressions have been found; to name the most relevant we have entanglement in $(2 \otimes 2)$ -dimensional systems [10], some families of states [11,12], and classical and quantum correlations [13–20]. If we consider the total quantum system made of two parts, then all correlations, both classical and quantum, can be defined as entropic quantities [21]. In what follows, we will define the total correlations by means of measures on one of the subsystems.

A bipartite quantum system $\hat{\rho}_{AB}$ can feature both quantum and classical correlations. Total correlations can be characterized by the quantum mutual information [21–25]

$$I(\hat{\rho}_{AB}) = S(\hat{\rho}_A) + S(\hat{\rho}_B) - S(\hat{\rho}_{AB}), \quad (1)$$

where $S(\hat{\rho}) = -\text{Tr}[\hat{\rho} \log_2(\hat{\rho})]$ is the von Neumann entropy. Based on this expression, it is commonly believed that the correlations can be separated according to their classical and quantum natures, respectively [21]. In this way, the quantum discord has been introduced as

$$D(\hat{\rho}_{AB}) = I(\hat{\rho}_{AB}) - C(\hat{\rho}_{AB}), \quad (2)$$

where $C(\hat{\rho}_{AB})$ are the classical correlations [21,22] defined by the following maximization procedure. A complete set of projector operators $\{\hat{\Pi}_k\}$ must be constructed for the subsystem B .

Then the quantity

$$C(\hat{\rho}_{AB}) = \max_{\{\hat{\Pi}_k\}} [S(\hat{\rho}_A) - S(\hat{\rho}_{AB}|\{\hat{\Pi}_k\})] \quad (3)$$

must be maximized with respect to variation of the set of $\{\hat{\Pi}_k\}$, where $S(\hat{\rho}_{AB}|\{\hat{\Pi}_k\}) = \sum_k p_k S(\hat{\rho}_k)$, $p_k = \text{Tr}(\hat{\rho}_{AB} \hat{\Pi}_k)$, and $\hat{\rho}_k = \text{Tr}_B(\hat{\Pi}_k \hat{\rho}_{AB} \hat{\Pi}_k) / p_k$.

In this paper, we investigate the dynamical evolution of classical correlations, using models for decoherence in the Markovian and non-Markovian regimes. Our main focus is to study the evolution of classical and quantum correlations in the case of a bipartite system, where each part is represented by a subsystem of dimension 3 or so-called qutrit. In Sec. II, we begin by introducing a general decoherence model from which the two regimes mentioned above can be obtained. These regimes can be implemented simply by making assumptions about the time given by the inverse of decay rates and correlation time of the reservoir. Also, we define the initial state for two qutrits using the discrete quantum Fourier transform. In Sec. III, we present a general basis in the qutrit Hilbert space where the maximization procedure can be carried out. Although its form is simple, it is worth mentioning that in the actual case the maximization procedure must be performed in a Bloch hypersphere defined by four angles. We specialize our analysis by studying three cases of interest: the Markovian case (Sec. III A), the non-Markovian case (Sec. III B), and the limit of long times (Sec. III C). We present analytic results for classical correlations, showing the apparition of stable and metastable pointer states. In Sec. IV, we present a summary.

II. QUANTUM DYNAMICS

We consider the dynamics of a bipartite system of qutrits under the onset of dephasing. In particular, each qutrit is defined as a quantum electromagnetic field mode having zero, one, or two excitations. That is, qutrits are defined in the terms of the Fock states $\{|0\rangle_{A(B)}, |1\rangle_{A(B)}, |2\rangle_{A(B)}\}$, where $|k\rangle_{A(B)}$ is the Fock state with k excitations in the quantum field mode A (B). Each field mode is coupled to a different reservoir and the interaction Hamiltonian will be given by $\hat{H} = \hat{H}_A + \hat{H}_B$,

where $\hat{H}_{A(B)}$ is the Hamiltonian describing the interaction of the quantum field mode A (B) with the reservoir R_A (R_B). The interactions have the form

$$\hat{H}_A = \sum_k \{g_k^A \hat{c}_k \hat{a}^\dagger \hat{a} + (g_k^A)^* \hat{c}_k^\dagger \hat{a}^\dagger \hat{a}\}, \quad (4)$$

$$\hat{H}_B = \sum_k \{g_k^B \hat{d}_k \hat{b}^\dagger \hat{b} + (g_k^B)^* \hat{d}_k^\dagger \hat{b}^\dagger \hat{b}\}, \quad (5)$$

where the operator \hat{a}^\dagger (\hat{b}^\dagger) creates a quantum of excitation of the field mode A (B) and \hat{a} (\hat{b}) are the corresponding annihilation operators. The operators \hat{c}_k^\dagger (\hat{d}_k^\dagger) create an excitation in the k th mode of the reservoir R_A (R_B), while \hat{c}_k and \hat{d}_k annihilate the excitation in the same reservoir mode. Coefficients g_k^A (g_k^B) are the coupling strength between the quantum field mode A (B) and the k th mode of the reservoir R_A (R_B). The types of interactions described in Eqs. (4) and (5) have been considered, for instance, to study the effects of the interaction with reservoirs on quantum decoherence [26]. The Hamiltonian $\hat{H} = \hat{H}_A + \hat{H}_B$ can be interpreted as a scattering process, for example, the dynamics of a photon scattering randomly as it travels through a waveguide, where the energy eigenstates do not evolve but accumulate phase instead. In this process, the information about relative phases between the eigenstates is lost [27,28].

The evolution of the quantum field modes subsystem can be obtained by solving the master equation

$$\begin{aligned} \dot{\hat{\rho}}_{AB} = & \frac{Q_A(t)}{2} [2\hat{a}^\dagger \hat{a} \hat{\rho}_{AB} \hat{a}^\dagger \hat{a} - (\hat{a}^\dagger \hat{a})^2 \hat{\rho}_{AB} - \hat{\rho}_{AB} (\hat{a}^\dagger \hat{a})^2] \\ & + \frac{Q_B(t)}{2} [2\hat{b}^\dagger \hat{b} \hat{\rho}_{AB} \hat{b}^\dagger \hat{b} - (\hat{b}^\dagger \hat{b})^2 \hat{\rho}_{AB} - \hat{\rho}_{AB} (\hat{b}^\dagger \hat{b})^2]. \end{aligned} \quad (6)$$

This master equation allows us to study two different regimes: Markovian and non-Markovian. To do this, we consider that the reservoirs present Ornstein-Uhlenbeck correlations, where [29]

$$Q_j(t) = \frac{\Gamma_j \gamma_j}{2} \left[\frac{\sin(\eta_j t)}{\eta_j \cos(\eta_j t) + (\gamma_j/2) \sin(\eta_j t)} \right],$$

where $1/\gamma_i$ is the correlation time of the reservoirs, Γ_i is the decay rate of the qutrit subsystem, and $\eta_i^2 = (\Gamma_i - \gamma_i/2)\gamma_i/2$. This time-dependent coefficient in the master equation arises if we consider, as developed in Ref. [29], a quasi-Lorentzian model for the coupling strengths g_k^A and g_k^B . Solving the master equation (6), we find that in the basis $\{|nm\rangle\}$, the density-matrix elements $\langle nk | \hat{\rho}_{AB} | ml \rangle \equiv \rho_{nk,ml}$ are given by

$$\rho_{nk,ml}(t) = \rho_{nk,ml}(0) P_A(t)^{|n-m|^2} P_B(t)^{|k-l|^2}, \quad (7)$$

where $n, m, k, l = 0, 1, 2, \dots, d-1$, with d the dimension of each system and

$$P_j(t) = e^{\beta_j t} \left(\cos(\eta_j t) - \frac{\beta_j}{\eta_j} \sin(\eta_j t) \right), \quad (8)$$

with $\beta_j = -\gamma_j/2$.

In order to study the evolution of quantum and classical correlations in higher-dimensional bipartite systems, the election of the initial state must ensure that the system is actually occupying more than two dimensions of the Hilbert space.

Here we consider an incoherent superposition of generalized Bell states for qutrits as follows:

$$\hat{\rho}_{AB}(0) = p_0 |\phi_{00}\rangle \langle \phi_{00}| + p_1 |\phi_{01}\rangle \langle \phi_{01}| + p_2 |\phi_{02}\rangle \langle \phi_{02}|. \quad (9)$$

The generalized Bell states are defined as

$$|\phi_{jk}\rangle = \hat{X}_{12} \hat{F}_1 |jk\rangle_{12}, \quad (10)$$

where \hat{X}_{12} is the XOR gate and is defined through $\hat{X}_{12} |j\rangle |k\rangle = |j\rangle |j \ominus k\rangle$, with $j \ominus k$ the difference between j and k modulus d , with d being the dimension of each system. The operator \hat{F} is the discrete quantum Fourier transform and is defined acting on the state $|j\rangle$, leading to $\hat{F} |j\rangle = (1/\sqrt{d}) \sum_{k=0}^{d-1} \exp(i2\pi jk/d) |k\rangle$. Notice that for $d=2$, \hat{X}_{12} is the controlled-NOT gate and the Fourier transform is the Hadamard gate. These two operators acting on the two-qubit basis $\{|00\rangle, |01\rangle, |10\rangle, |11\rangle\}$ generate all four Bells states for two-qubit systems. Now for qutrits ($d=3$), from Eq. (10) we have that

$$|\phi_{00}\rangle = \frac{1}{\sqrt{3}} (|00\rangle + |11\rangle + |22\rangle),$$

$$|\phi_{01}\rangle = \frac{1}{\sqrt{3}} (|02\rangle + |10\rangle + |21\rangle),$$

$$|\phi_{02}\rangle = \frac{1}{\sqrt{3}} (|01\rangle + |12\rangle + |20\rangle).$$

III. QUANTUM AND CLASSICAL CORRELATION DYNAMICS

To calculate the evolution of quantum and classical correlations in our qutrit system, we have to choose a general set of three orthogonal states. This set must be constructed in such a way that the measurement projectors cover the complete Bloch sphere. Furthermore, as measurements can be performed on either qutrit, we must choose one of them. Here, for instance, classical correlations will be calculated by performing measurements on qutrit B . For that, we consider the basis [30]

$$|V_1\rangle = e^{i\chi_1} \sin \theta \cos \phi |0\rangle + e^{i\chi_2} \sin \theta \sin \phi |1\rangle + \cos \theta |2\rangle,$$

$$|V_2\rangle = e^{i\chi_1} \cos \theta \cos \phi |0\rangle + e^{i\chi_2} \cos \theta \sin \phi |1\rangle - \sin \theta |2\rangle,$$

$$|V_3\rangle = -e^{i\chi_1} \sin \phi |0\rangle + e^{i\chi_2} \cos \phi |1\rangle,$$

where the ranges for the angles are $(0 \leq \theta, \phi \leq \pi/2)$ and $(0 \leq \chi_1, \chi_2 \leq 2\pi)$. Using this basis, we can evaluate the expression for classical correlations given in Eq. (3). Although it has been argued that more general measurements should be considered to calculate classical correlations, it has been shown that this generates only minimal corrections to the calculations using projective measurements [31].

In the following, we will study the quantum and classical correlations in both Markovian and non-Markovian regimes.

A. Markovian regime

The Markovian regime is recovered when the reservoir correlation time becomes much smaller than the system decay time ($\Gamma_j \ll \gamma_j$). In this limit, it can be shown that $P(t)_j \approx e^{-\Gamma_j t/2}$ and the density-matrix elements of Eq. (7)

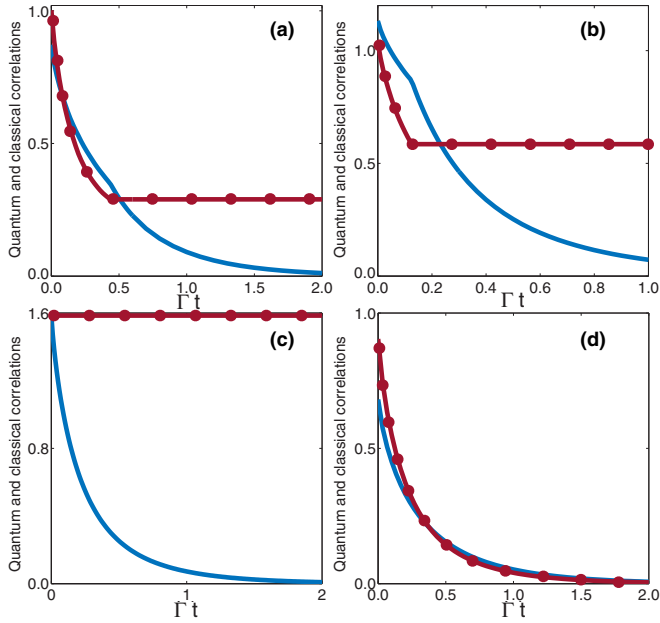


FIG. 1. Evolution of discord $D(\hat{\rho}_{AB})$ (blue solid line) and classical correlations $C(\hat{\rho}_{AB})$ (red dotted line) for the initial state of Eq. (9) with the parameters (p_0, p_1, p_2) with values (a) $(0.3, 0.1, 0.6)$, (b) $(0, 0.5, 0.5)$, (c) $(0, 0, 1)$, and (d) $(1/3, 1/3, 1/3)$. For simplicity we consider $\Gamma_1 = \Gamma_2 = \Gamma$.

reduce to

$$\rho_{nk,ml}(t) = \rho_{nk,ml}(0) \exp \left[-\frac{1}{2}(\Gamma_1 |n - m|^2 + \Gamma_2 |k - l|^2)t \right]. \quad (11)$$

The evolution of quantum and classical correlations for this density matrix are shown in Fig. 1 for the initial state of Eq. (9), for four different sets of parameters p_0 , p_1 , and p_2 . Figure 1(a) corresponds to the case with different values of the parameters ($p_0 = 0.3$, $p_1 = 0.1$, and $p_2 = 0.6$). Interestingly, we observe in this case that, until a given (finite) time Γt , the classical correlations decay. Then it freezes to an stationary value while quantum discord decays asymptotically to zero. In previous works [5,7,9], similar behavior was found in the two-qubit scenario where the classical correlation also exhibits a sudden change in its dynamics accompanied by a sudden change in the discord dynamics. However, this is no longer true in our case since the quantum discord decay at all times. This can be interpreted as the decoherence dynamics exhibiting two regimes: a mixed one, where decoherence has a quantum and a classical contribution, i.e., both correlations decay, and a second regime where the decoherence has only quantum character. In the latter regime, only the quantum correlations decay.

Although the evolution of correlations is similar, in Fig. 1(b) we observe that for a different set of parameters ($p_0 = 0$, $p_1 = 0.5$, and $p_2 = 0.5$) the stationary value of the classical correlations is considerably higher compared to the case in Fig. 1(a). This becomes more apparent when we consider an initial state with parameters $p_0 = p_1 = 0$ and $p_2 = 1$. This particular state corresponds to a pure initial state whose quantum and classical correlations evolve as shown in Fig. 1(c). Interestingly, the classical correlations for this state are not

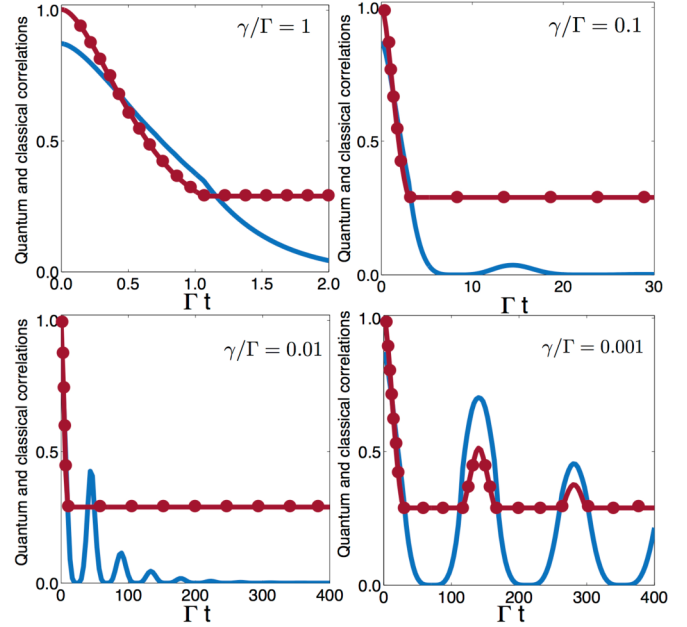


FIG. 2. Evolution of discord $D(\hat{\rho}_{AB})$ (blue solid line) and classical correlations $C(\hat{\rho}_{AB})$ (red dotted line) for the initial state of Eq. (9) with $(p_0, p_1, p_2) = (0.3, 0.1, 0.6)$ for different values of γ/Γ .

affected by decoherence and stay constant along the dynamics, while the quantum discord decays asymptotically to zero as expected.

The sudden change in the classical correlations depicted in Figs. 1(a) and 1(b) reveals the apparition of a pointer state associated with the system being measured as have been encountered in previous works [7,9]. The stationary value reached by the classical correlations tells us that, by measuring on the system B , we will obtain the same information about the A at all times and the measurement operators are defined on the basis of classical states that are not affected by decoherence [7]. In other words, we observe that after a finite time, the system settles on a stable pointer-state basis.

On the other hand, in Fig. 1(d) we show the case with $p_0 = p_1 = p_2 = 1/3$. Interestingly, for equal parameters in the initial state, the classical correlations show a different behavior compared to the previous ones: It decays asymptotically to zero as well as the quantum discord. That is, for a balanced incoherent superposition in the initial state (9), the systems does not reach a pointer state. Numerically we have observed that whichever the combination of p_j 's is, we always found a nonzero stationary value for classical correlations with the only exception of $p_0 = p_1 = p_2 = 1/3$.

B. Non-Markovian regime

In this regime we consider the cases when $\Gamma \sim \gamma$ and $\Gamma \gg \gamma$. This relation between coherence times for reservoirs and qutrits allows the quantum system to exhibit a richer dynamics and, in consequence, quantum and classical correlations show features that cannot be observed under the Markov approximation. For example, in Fig. 2 we show the evolution of quantum and classical correlations considering the initial

state (9) with $p_0 = 0.3$, $p_1 = 0.1$, and $p_2 = 0.6$ for different values of γ .

When $\gamma = \Gamma$, we observe in the figure that the dynamics is similar to that found in the Markovian case shown in Fig. 1(a). However, at short times the characteristic nonexponential behavior of the non-Markovian regime is present. In this case, a pointer state also emerges, as evidenced by the frozen classical correlations.

As the value of γ decreases in relation to Γ , the non-Markovian behavior becomes more evident: For $\gamma = 0.1\Gamma$, on one hand, we observe that quantum discord decays asymptotically to zero and after a given time, a revival is observed, followed again by an asymptotic decay. On the other hand, the classical correlations show similar behavior in Figs. 1(a) and 1(b). This reveals an interesting regime where quantum correlations exhibit non-Markovian dynamics [32] while classical correlations evolve within a Markovian frame. Now, when $\gamma = 0.01\Gamma$ this mixed non-Markovian and Markovian behavior of quantum and classical correlations is still present with the only difference that quantum correlations exhibit more revivals before disappearing completely.

In the last case $\gamma = 0.001\Gamma$ the amplitude of the quantum discord revivals increases, but its behaviors remains similar to previous cases. Interestingly, this is not true for classical correlations whose evolution experiences significant differences from all previous cases (Markovian and non-Markovian) considered. Although the system settles on a pointer-state basis, this basis is no longer stable. Indeed, we observe the emergence of metastable pointer states as previously found in Ref. [9].

Up to this point, we have only considered discord as a measure of quantum correlations and not, for example, entanglement. The reason is that quantum entanglement, quantified through the EOF, has no closed formula for general mixed density matrices and its calculation is numerically more challenging than for discord. However, there is a lower bound of EOF that can be calculated directly [33] and also the negativity \mathcal{N} [34] can be considered as an estimator of entanglement. The lower bound of EOF for a two-qutrit bipartition is given by

$$E(\hat{\rho}) \geq \begin{cases} 0 & \text{if } \Lambda = 1 \\ H_2[\gamma(\Lambda)] + [1 - \gamma(\Lambda)] & \text{if } \Lambda \in [1, 8/3] \\ (\Lambda - 3) + \log_2(3) & \text{if } \Lambda \in [8/3, 3], \end{cases} \quad (12)$$

where $\gamma(\Lambda) = [\sqrt{\Lambda} + \sqrt{2(3 - \Lambda)}]^2/9$, with $\Lambda = \max[\|\hat{\rho}^{T_A}\|, \|R(\hat{\rho})\|]$ and $H_2(x) = -x \log_2(x) - (1 - x) \log_2(1 - x)$. The trace norm $\|\cdot\|$ is defined as $\|G\| = \text{tr}(GG^\dagger)^{1/2}$. The matrix ρ^{T_A} is the partial transpose with respect to the subsystem A , that is, $\rho_{ik,jl}^{T_A} = \rho_{jk,il}$, and the matrix $R(\rho)$ is defined as $R(\rho)_{ij,kl} = \rho_{ik,jl}$. On the other hand, the negativity [34] is given by $\mathcal{N} = (\|\rho^{T_A}\| - 1)/2$. Figure 3 shows a comparison among the lower bound of EOF, the negativity \mathcal{N} , discord, and classical correlations for the non-Markovian case $\gamma/\Gamma = 0.001$. Although we observe that both the lower bound of EOF (green line) and the negativity (black-dashed line) evolve in a similar fashion than quantum discord (blue line), they suffer periodical *sudden deaths* [35] along its dynamics. Abrupt changes in the entanglement

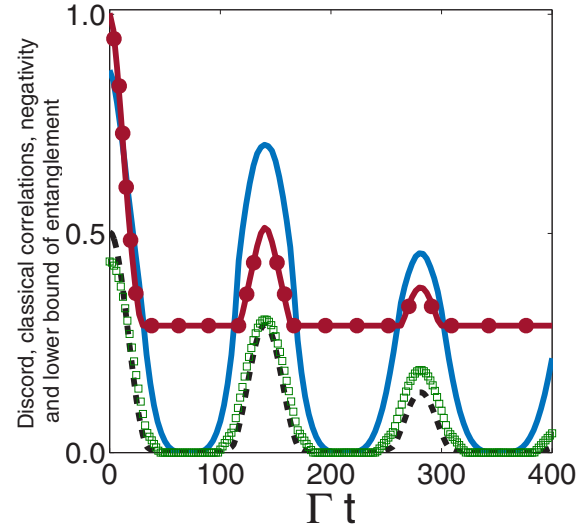


FIG. 3. Evolution of discord $D(\hat{\rho}_{AB})$ (blue solid line), classical correlations $C(\hat{\rho}_{AB})$ (red dotted line), the lower bound of entanglement of formation (green squares) [33] and negativity $\mathcal{N} = (\|\rho_A^T\| - 1)/2$ (black dashed line) for the initial state of Eq. (9) with $(p_0, p_1, p_2) = (0.3, 0.1, 0.6)$ and $\gamma/\Gamma = 0.001$.

dynamics have also been found in initially mixed states of qutrits in a dissipative dynamics [36].

C. Long-time limit

The optimization process required to calculate the classical correlations defined in Eq. (3) makes the search for analytical expressions of $C(\rho_{AB})$ a difficult task to realize in general. For instance, in qutrits this has been made numerically only [37]. However, in our physical system of two noninteracting qutrits each under dephasing, the classical correlations can be calculated analytically when $t \rightarrow \infty$. After some calculations, we find that

$$C(t \rightarrow \infty) = \max_{[\theta, \phi]} f(\theta, \phi), \quad (13)$$

where

$$f(\theta, \phi) = -\log_2(1/3) + (1/3) \sum_{j=1}^9 \lambda_j \log_2(\lambda_j), \quad (14)$$

with

$$\begin{aligned} \lambda_{1,2,3} &= \{x \cos^2(\theta) + \sin^2(\theta)[y \cos^2(\phi) + z \sin^2(\phi)]\}, \\ \lambda_{4,5,6} &= \{x \sin^2(\theta) + \cos^2(\theta)[y \cos^2(\phi) + z \sin^2(\phi)]\}, \\ \lambda_{7,8,9} &= \frac{1}{2}[1 - x + (y - z) \cos(2\phi)], \end{aligned}$$

where (x, y, z) is (p_0, p_1, p_2) , (p_1, p_2, p_0) , and (p_2, p_0, p_1) .

As we see from the expressions above, in the long-time limit $t \rightarrow \infty$, classical correlations depend only on the angles θ and ϕ , rather than the four original parameters defined by the orthonormal basis $\{|V_1\rangle, |V_2\rangle, |V_3\rangle\}$ previously defined. Figure 4 shows the function $f(\theta, \phi)$ from which the classical correlations are calculated [Eq. (13)]. It is clear in Fig. 4 that the maximum value of this function is found at four different sets of angles (θ, ϕ) . The four points correspond to the following

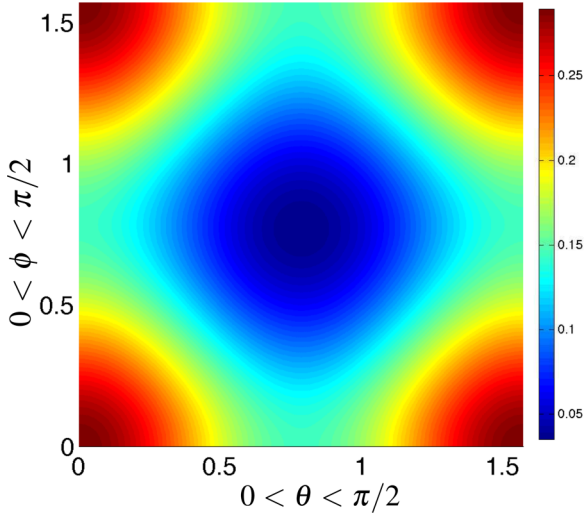


FIG. 4. Function $f(p_0, p_1)$ using the normalization constraint $p_2 = 1 - (p_0 + p_1)$, which for each value of p_0, p_1 we have performed the maximization over θ and ϕ .

sets of angles: $(\theta = 0, \phi = 0)$, $(\theta = \pi/2, \phi = 0)$, $(\theta = 0, \phi = \pi/2)$, and $(\theta = \pi/2, \phi = \pi/2)$. Therefore, using these results, we can reconstruct the basis from which classical correlations are obtained. For instance, from the set $(\theta = 0, \phi = 0)$ we have

$$\begin{aligned} |V_1\rangle &= |2\rangle, \\ |V_2\rangle &= e^{i\chi_1}|0\rangle, \\ |V_3\rangle &= e^{i\chi_2}|1\rangle. \end{aligned} \quad (15)$$

Notice that the angles χ_1 and χ_2 may take any value in the interval $(0 \leq \chi_1, \chi_2 \leq 2\pi)$ without changing the value for the classical correlations. This result allows us to calculate analytically the classical correlations in the long-time limit, as

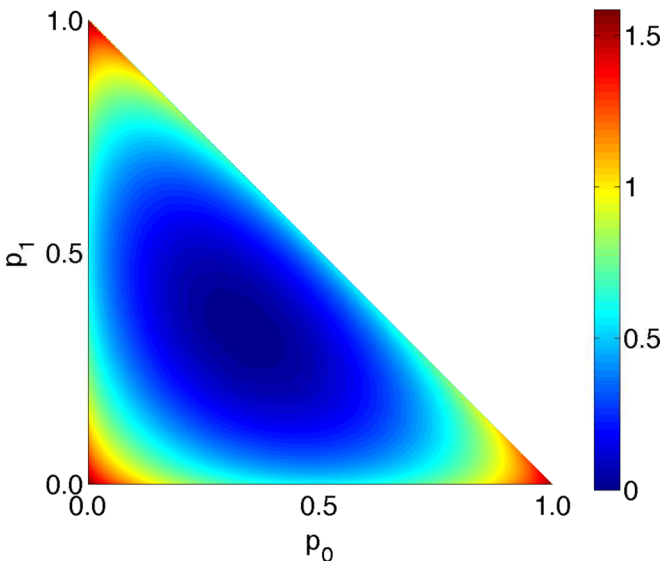


FIG. 5. Stationary classical correlations $C(\hat{\rho}_{AB})$ in the long-time limit as a function of (p_0, p_1) .

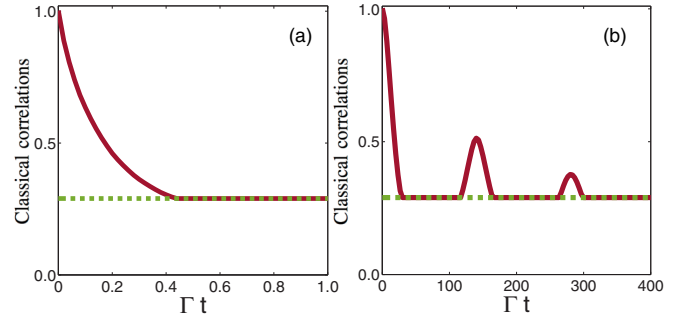


FIG. 6. Classical correlations calculated using the general form of Eq. (3) (red solid line) and considering the measurement on the second qutrit performed in the basis analytically found in Eq. (15) (green dashed line) in the (a) Markovian regime and (b) non-Markovian case with $\gamma/\Gamma = 0.001$. Initial states correspond to Eq. (9) with $(p_0, p_1, p_2) = (0.3, 0.6, 0.1)$.

a function of the initial-state parameters (p_0, p_1, p_2) , as shown in Fig. 5. The stationary behavior of classical correlations shown in Fig. 5 is in agreement with the previous findings shown in Fig. 1. For example, the maximum stationary values of classical correlations found, p_0 , p_1 , or p_2 , are equal to 1, that is, a pure initial state, as shown in Fig. 1(c). On the other hand, minimum values for frozen classical correlations are observed for a balanced superposition in the initial state $p_0 = p_1 = p_2 = 1/3$, whose dynamics is shown in Fig. 1(d).

Although Markovian and non-Markovian regimes show important differences in the quantum dynamics of the system, as well as in the behavior of quantum and classical correlations, we found from our calculations that the settling of the system on the pointer-state basis does not depend on the relation between the coherence times of the reservoir and the decay rate of the qutrits. In the Markovian regime, we see in Fig. 6(a) the classical correlations calculated using the general form of Eq. (3) together with the classical correlations obtained analytically. This figure shows us that the system settles on the pointer-state basis found in the long-time limit, long before this limit is actually reached. This is also the case when the non-Markovian regime is considered [Fig. 6(b)]; even though the settling might be unstable, at the end it reaches the same expected pointer-state basis. Interestingly, the set of vectors defining the pointer-state basis consists of the eigenvectors of the observable \hat{S}_z with spin $s = 1$. This analytical result is in agreement with what was observed in previous works that showed that eigenvectors of \hat{S}_z with spin $s = 1/2$ maximize classical correlations for qubits [7,9,18].

IV. CONCLUSION

In summary, we have studied the dynamics of quantum and classical correlations in a two-qutrit system under the onset of dephasing. In the Markovian regime, we observed that the decoherence process can be characterized by considering two different regimes: one where both classical and quantum correlations are affected by the decoherence and another where only quantum correlations decay while classical correlations remain constant. This can be understood as the measurement basis projecting the measured qutrit into classical states

(pointer states) that are not affected by decoherence. We showed in the long-time limit that this observable corresponds to the spin operator \hat{S}_z with spin $s = 1$, consistent with previous similar results for the two-qubit case where the same operator but with spin $s = 1/2$ was found. On the other hand, we found more varied results as a function of the ratio γ/Γ . For example, we found for $\gamma/\Gamma \ll 1$ that the non-Markovianity is reflected

in the classical correlations by the apparition of metastable pointer states.

ACKNOWLEDGMENT

C.E.L. acknowledges support from DICYT Grant No. 041631LC.

-
- [1] E. Joos, H. D. Zeh, C. Kiefer, D. J. W. Giulini, J. Kupsch, and I.-O. Stamatescu, *Decoherence and the Appearance of a Classical World in Quantum Theory* (Springer Science & Business Media, New York, 2003).
- [2] H.-P. Breuer and F. Petruccione, *The Theory of Open Quantum Systems* (Oxford University Press, Oxford, 2002).
- [3] W. H. Zurek, *Ann. Phys. (Leipzig)* **9**, 855 (2000).
- [4] W. H. Zurek, *Rev. Mod. Phys.* **75**, 715 (2003).
- [5] L. Mazzola, J. Piilo, and S. Maniscalco, *Phys. Rev. Lett.* **104**, 200401 (2010).
- [6] J.-S. Xu, C.-F. Li, C.-J. Zhang, X.-Y. Xu, Y.-S. Zhang, and G.-C. Guo, *Phys. Rev. A* **82**, 042328 (2010).
- [7] M. F. Cornelio, O. J. Farías, F. F. Fanchini, I. Frerot, G. H. Aguilar, M. O. Hor-Meyll, M. C. de Oliveira, S. P. Walborn, A. O. Caldeira, and P. H. S. Ribeiro, *Phys. Rev. Lett.* **109**, 190402 (2012).
- [8] F. M. Paula, I. A. Silva, J. D. Montealegre, A. M. Souza, E. R. deAzevedo, R. S. Sarthour, A. Saguia, I. S. Oliveira, D. O. Soares-Pinto, G. Adesso, and M. S. Sarandy, *Phys. Rev. Lett.* **111**, 250401 (2013).
- [9] F. Lastra, C. E. López, S. A. Reyes, and S. Wallentowitz, *Phys. Rev. A* **90**, 062103 (2014).
- [10] W. K. Wootters, *Phys. Rev. Lett.* **80**, 2245 (1998).
- [11] B. M. Terhal and K. G. H. Vollbrecht, *Phys. Rev. Lett.* **85**, 2625 (2000).
- [12] R. Horodecki, P. Horodecki, M. Horodecki, and K. Horodecki, *Rev. Mod. Phys.* **81**, 865 (2009).
- [13] S. Luo, *Phys. Rev. A* **77**, 042303 (2008).
- [14] M. Ali, A. R. P. Rau, and G. Alber, *Phys. Rev. A* **81**, 042105 (2010); **82**, 069902(E) (2010).
- [15] G. Karpat and Z. Gedik, *Phys. Lett.* **47A**, 4166 (2011).
- [16] E. Chitambar, *Phys. Rev. A* **86**, 032110 (2012).
- [17] M. Ali, *J. Phys. A: Math. Theor.* **43**, 495303 (2010).
- [18] Q. Chen, C. Zhang, S. Yu, X. X. Yi, and C. H. Oh, *Phys. Rev. A* **84**, 042313 (2011).
- [19] S. Khan and M. K. Khan, *J. Mod. Opt.* **58**, 918 (2011).
- [20] S. Khan and I. Ahmad, *Optik* **127**, 2448 (2016).
- [21] H. Ollivier and W. H. Zurek, *Phys. Rev. Lett.* **88**, 017901 (2001).
- [22] L. Henderson and V. Vedral, *J. Phys. A* **34**, 6899 (2001).
- [23] V. Vedral, *Rev. Mod. Phys.* **74**, 197 (2002).
- [24] B. Groisman, S. Popescu, and A. Winter, *Phys. Rev. A* **72**, 032317 (2005).
- [25] B. Schumacher and M. D. Westmoreland, *Phys. Rev. A* **74**, 042305 (2006).
- [26] D. F. Walls and G. J. Milburn, *Phys. Rev. A* **31**, 2403 (1985).
- [27] C. W. Gardiner, *Quantum Noise* (Springer, Berlin, 1991).
- [28] M. A. Nielsen and I. L. Chuang, *Quantum Computation and Quantum Information* (Cambridge University Press, Cambridge, 2000).
- [29] C. J. Broadbent, J. Jing, T. Yu, and J. H. Eberly, *Ann. Phys. (NY)* **327**, 1962 (2012).
- [30] C. M. Caves and G. J. Milburn, *Opt. Commun.* **179**, 439 (2000).
- [31] F. Galve, G. L. Giorgi, and R. Zambrini, *Europhys. Lett.* **96**, 40005 (2011).
- [32] A. Rivas, S. F. Huelga, and M. B. Plenio, *Phys. Rev. Lett.* **105**, 050403 (2010).
- [33] K. Chen, S. Albeverio, and S.-M. Fei, *Phys. Rev. Lett.* **95**, 210501 (2005).
- [34] G. Vidal and R. F. Werner, *Phys. Rev. A* **65**, 032314 (2002).
- [35] T. Yu and J. H. Eberly, *Phys. Rev. Lett.* **93**, 140404 (2004); **97**, 140403 (2006).
- [36] F. Lastra, G. Romero, C. E. López, M. F. Santos, and J. C. Retamal, *Phys. Rev. A* **75**, 062324 (2007).
- [37] F. A. Cárdenas-López, S. Allende, and J. C. Retamal, *Sci. Rep.* **7**, 44654 (2017).